

PARTICLE-IN-CELL SIMULATION OF A BUNCHED ELECTRONS BEAM ACCELERATION IN A TE_{113} CYLINDRICAL CAVITY AFFECTED BY A STATIC INHOMOGENEOUS MAGNETIC FIELD*

E. A. Orozco[†], Universidad Industrial de Santander, A.A. 678 Bucaramanga, Colombia

V. E. Vergara, J. D. González, J. R. Beltrán,

Universidad del Magdalena, A.A.731 Santa Marta, Colombia

Abstract

The results of the relativistic full electromagnetic Particle-in-cell (PIC) simulation of a bunched electrons beam accelerated in a TE_{113} cylindrical cavity in the presence of a static inhomogeneous magnetic field are presented. This type of acceleration is known as Spatial AutoResonance Acceleration (SARA). The magnetic field profile is such that it keeps the electrons beam in the acceleration regime along their trajectories. Numerical experiments of bunched electrons beam with the concentrations in the range 10^8 – 10^9 cm $^{-3}$ in a linear TE_{113} cylindrical microwave field of a frequency of 2.45 GHz and an amplitude of 15 kV/cm show that it is possible accelerate the bunched electrons up to energies of 250 keV without serious defocalization effect. A comparison between the data obtained from the full electromagnetic PIC simulations and the results derived from the relativistic Newton-Lorentz equation in a single particle approximation is carried out. This acceleration scheme can be used as a basis to produce hard x-ray.

INTRODUCTION

The last decades, particle accelerators based on the electron cyclotron resonance (ECR) phenomenon has been extensively studied. Different technological applications based on this phenomenon has been proposed [1–5]. There are different ways to maintain the ECR condition, which use: (i) Transversal electromagnetic (TEM) waves in a homogeneous magnetostatic field [6, 7], (ii) Transversal electric (TE) waves in waveguides placed on inhomogeneous magnetostatic field [8, 9], (iii) TE standing electromagnetic waves in cavities affected by a homogeneous magnetic field growing slowly in time, known as GYRAC [10, 11] or (iv) TE standing electromagnetic waves in cavities affected by an inhomogeneous magnetostatic field, known as SARA [12–16]; among others [17]. In the SARA concept the magnetostatic field is fitted along the resonant cavity axis to keep the ECR acceleration regime as the electrons move in helical trajectories. The SARA concept has been studied both analytically and numerically in cylindrical TE_{11p} cavities [12–15] as well as in a TE_{112} rectangular cavities [16]. An X ray source based on the SARA concept has been certificated [18].

In the present paper, the influence of the self-consistent field on the space autoresonance acceleration (SARA) of

bunched electrons beams in the linear TE_{113} cylindrical cavity is analized, by using a full electromagnetic relativistic particle-in-cell code. In our numerical scheme, the simulation is carried out in two stages:

1. Calculation of the TE_{113} steady-state microwave field before injecting the electrons bunched
2. Self-consistent simulation of the bunched electrons beams in the SARA acceleration.

The cylindrical TE_{113} cavity, whose radius and length are 4.54 cm and 30 cm respectively, is excited by a 2.45 GHz source. In our numerical model, to excite the TE_{113} microwave field of 15 kV/cm tension, an input power of 728 kW is injected into the cavity through a TE_{10} waveguide. The electron's bunched, whose concentrations are in the range 10^8 – 10^9 cm $^{-3}$, are described in the framework of the Vlasov-Maxwell equation; which is solved numerically through the particle-in-cell (PIC) method [19].

The obtained results show that it is possible accelerate bunched electrons up to energies of 260 keV without serious defocalization effect. A comparison between the data obtained from the full electromagnetic PIC simulations and the results derived from the relativistic Newton-Lorentz equation in a single particle approximation [15] is carried out. This acceleration scheme can be used as a basis to produce hard x-ray.

THEORETICAL FORMALISM AND NUMERICAL METHOD

Physical Scheme and Theoretical Formalism

The electron acceleration in the autoresonance regime by a standing transversal electric microwave field in an inhomogeneous magnetostatic field, known as *Spatial AutoResonance Acceleration (SARA)*, can be realized in the physical system shown in Fig. 1.

The cylindrical cavity 1 is placed inside the current coil set 2 that produces an azimuthally symmetric magnetostatic field whose value at the end where is the electron gun 5 is the corresponding to obtain classical resonance. The magnetostatic field profile has a relation with the used TE_{11p} ($p = 1, 2, 3, \dots$) mode 4, which is excited through the microwave port 3. The electrons gun 5 injects electrons by one end of the cavity 1 along the magnetostatic field axis, taken as z axis. The right-hand polarized electric field component of the microwave field accelerates the electrons by electron

* Work supported by Universidad Industrial de Santander (Colombia) and Universidad del Magdalena (Colombia)

[†] eaorozco@uis.edu.co

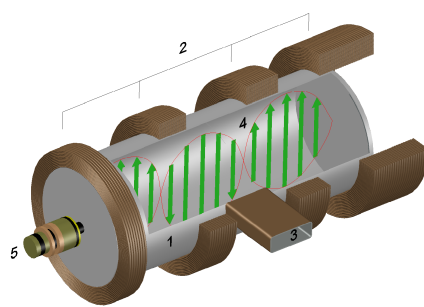


Figure 1: A physical model scheme. 1) cavity, 2) magnetic coils, 3) microwave port, 4) electric field profile; the particular case of TE_{113} mode, 5) electron gun.

cyclotron resonance (ECR) along their helical paths until they impact the opposite end of the cavity.

For a single particle and by using the paraxial approximation for the fields, the local electron cyclotron frequency $\omega_c(\vec{r})$ in the SARA concept is given by [12]:

$$\begin{aligned} \omega_c(z)/\omega &= \gamma^{-1} B_z(0, z)/B_0 \\ &+ \gamma^{-1} (E_0^c/B_0 c)[1 - \gamma^{-2} + (v_z/c)^2]^{-1/2} \\ &\times |\sin(p\pi z/L_c)| \sin \varphi \end{aligned} \quad (1)$$

where, ω is the microwave field frequency; γ is the Lorentz factor; $B_z(0, z)$ is the magnetostatic field profile along the cavity axis, whose value at the injection point is $\gamma_0 B_0$, being γ_0 the Lorentz factor in said point and $B_0 = m_e \omega/e$ is the magnetic field to obtain classical resonance (m_e and e are the mass and electric charge of the electron, respectively); E_0^c is the tension of the right-hand circular polarized component of the electric microwave field; c is the speed of light; v_z is the longitudinal component of electron velocity; p the index of the TE_{11p} mode; z the longitudinal coordinate of the electron; L_c the length of the cavity and finally, φ is the phase-shift between the electron transversal velocity and the electric field component of the microwave field.

A continuous sustenance of the exact resonance is possible only in the particular case of $p = 1$, because, if $p \neq 1$, the phase-shift φ jumps an angle π in each node of the standing electromagnetic wave. For the exact resonance $\varphi = \pi$, equation (1) leads to

$$\omega_c(z) = e B_z(0, z) / \gamma m_e \quad (2)$$

Therefore; to maintain the resonance condition $\omega = \omega_c$, the magnetostatic field has to be fitted to compensate the increasing of the relativistic factor as the electrons gain energies along its helical paths. In this case the magnetostatic field grows monotonously (see Fig. 2a).

For the case $p \neq 1$, the magnetostatic field grows in a non-monotonous way, which has to be fitted to maintain the phase-shift φ in the range $\pi < \varphi < 3\pi/2$ (see the case $p = 2$ in Fig. 2b). This range was named *Acceleration Band* because for these φ values the electromagnetic field can

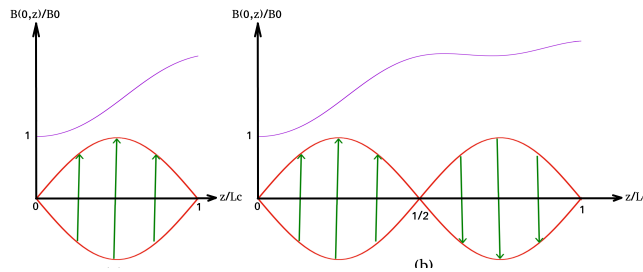


Figure 2: Typical magnetostatic field profiles (purple lines) used in the SARA concept for the modes (a) TE_{111} and (b) TE_{112} .

transfers energy to the electrons [12]. It is worth mentioning that in the SARA concept there is present the diamagnetic force, which is one of the important factors limiting the energy which can be achieved in this acceleration mechanism. In order to analyze the influence of the space-charge on the acceleration efficiency, a self-consistent simulation should be considered; being the Particle-in-cell (PIC) the most popular method used for the electrons beam simulations [19].

Numerical Method

To simulate the proposed system, a numerical scheme based on two sequential stages is used:

1. Calculation of the steady state for the microwave field before to inject the electrons beam
2. Self-consistent simulation of the bunched electrons beams in the SARA acceleration by the TE_{113} cylindrical microwave field

In our simulations, the perfect electric conductor (PEC) boundary conditions for both the cavity and the waveguide coupled to the microwave port are used. To avoid nonphysical reflections, a perfectly matched layer (PML) in the opposite end of said waveguide is used (see Fig. 3). To simulate the input power, the TE_{10} mode is excited in a plane adjacent to the PML into the rectangular waveguide (see Fig. 3). In order to calculate the electric and magnetic field on the mesh points we use the Uniaxial perfectly Matched Layer (UPML) method; which solve the Maxwell equations in a finite difference time domain (FDTD) scheme based on a Yee's cell for systems including PML [20, 21].

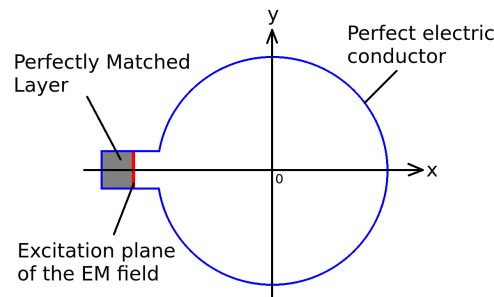


Figure 3: Waveguide-resonant cavity cross section.

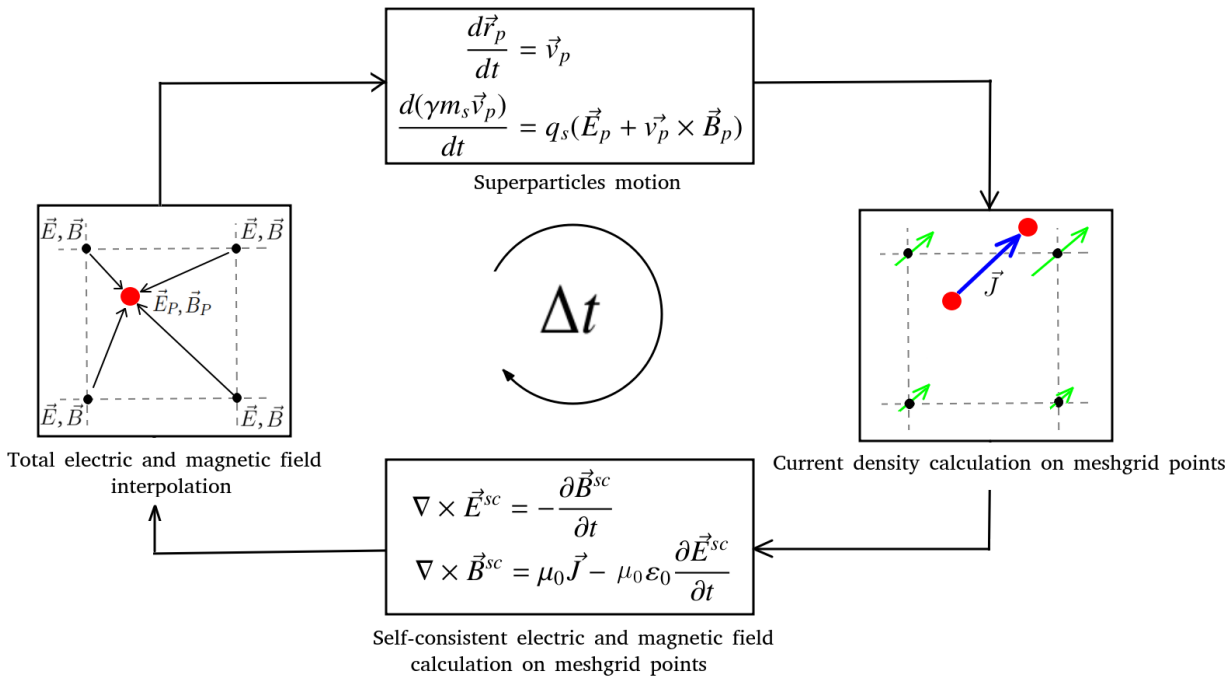


Figure 4: Electromagnetic PIC-algorithm.

For the second stage, the full electromagnetic particle-in-cell (PIC) method is used. In this method, groups of particles close to each other in the phase-space called superparticles (SP), are used to describe the evolution of the distribution function $f_e(\vec{r}, \vec{v}, t)$ [19].

The electromagnetic PIC-algorithm in a computational cycle is showed in Fig. 4, which involves the following steps:

- Calculation of the current densities in the mesh points (green arrows) from the superparticles (SP) positions and velocities data (blue arrow). In the present work, the current density is calculate using the conservative charge method proposed by Umeda et al in order to fulfill the continuity equation [22].
- Calculation of the self-consistent field on the mesh-grid points from the current density. In the present work, $\vec{E}^{sc} = \vec{E}^{hf} + \vec{E}^{sg}$, where \vec{E}^{hf} is the microwave electric field component and \vec{E}^{sg} is the self-generated electric field by the electrons bunch. Similarly, the self-consistent magnetic field component, \vec{B}^{sc} , is defined.
- Calculation of the total fields, \vec{E}_p and \vec{B}_p , acting on the superparticles. These fields are calculated through the interpolation of the total fields on the mesgrid points (see Fig. 4). In the present work, $\vec{E} = \vec{E}^{sc}$ and $\vec{B} = \vec{B}^{sc} + \vec{B}^s$, where \vec{B}^s is the magnetostatic field showed in Fig. 5.
- Calculation of new positions and velocities of the SPs through integration of their equations of motion. For this step, the relativistic Newton-Lorentz equation is

solved numerically through the Boris leapfrog procedure.

In our numerical simulations we consider a 2.45 GHz cylindrical cavity, whose radius and length are 4.54 cm and 30 cm respectively. To excite a microwave field of 15 kV/cm tension, an input power of 728 kW is injected into the cavity through a TE_{10} rectangular waveguide. It is worth mentioning that such high level of the microwave power is because a non-optimized microwave injection system has been used.

The magnetostatic field profile shown in Fig. 5, where $B_0 (= m_e \omega / e) = 0.0875$ T, is generated by four axisymmetric coils whose parameters are given in Table 1, where R_i ,

Table 1: Magnetic Coil System Parameters

Coil	R_i	R_e	L_b	J	z
1	6 cm	20 cm	6 cm	1.39 A/mm ²	-5.75 cm
2	6 cm	20 cm	7.5 cm	1.08 A/mm ²	8.25 cm
3	6 cm	20 cm	6.9 cm	1.18 A/mm ²	19.5 cm
4	6 cm	20 cm	6.1 cm	2.07 A/mm ²	32 cm

R_e , L_b , and z are the internal radius, the external radius, the width of each coil, and the positions of the coils, respectively, and J is the coil current density.

In order to analyze the influence of the space charge on the spatial autoresonance acceleration, simulations with spherical electrons bunches were carried out and divided in two cases (see Table 2).

The simulations are considered finished when the electrons impact with the cavity.

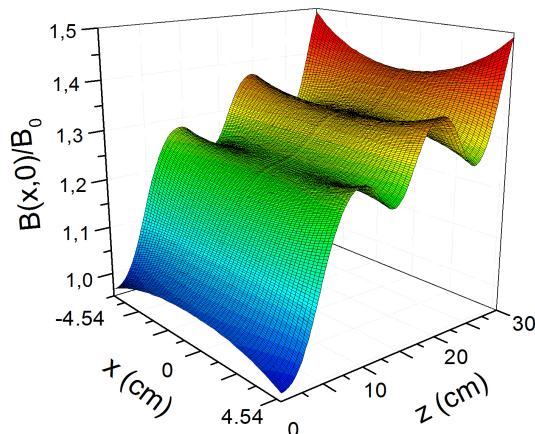


Figure 5: The profile of the magnetostatic field in the $y = 0$ plane.

Table 2: Parameters of the Simulations

	case 1	case 2
Beam parameters		
Electron Bunch Radius	0.5 cm	0.5 cm
Electron concentration	$n_e = 10^8 \text{ cm}^{-3}$	$n_e = 10^9 \text{ cm}^{-3}$
Injection energy	30 keV	32 keV
Simulation parameters		
Δx	0.07 cm	0.07 cm
Δy	0.07 cm	0.07 cm
Δz	0.3 cm	0.3 cm
Δt	1.58 ps	1.58 ps
PiC merging factor	2×10^4	2×10^5

RESULTS AND DISCUSSION

Figure 6 shows the obtained steady-state electric field distribution in the cross section $z = L_c/2$ (see Fig. 6a), the longitudinal plane $y = 0$ (see Fig. 6b) and the longitudinal plane $x = 0$ (see Fig. 6c) for the first stage of the simulation. This graphics show good agreement with the obtained from the well known analytical expressions of the linear polarized TE_{113} mode whose amplitude is $E_0^l = 15 \text{ kV/cm}$. The electrons interact effectively only with the right-hand polarized electric field component of the microwave field, which has an amplitude $E_0^c = E_0^l/2$. Figure 7 shows the time evolution of the phase-shift between the electrons transversal velocities and the right-hand circular polarized component of the electric microwave field, for the case 1 (see Table 2) and for the single-particle approximation studied in [15]. In this graph, the *Acceleration band* is shown in blue color.

It can be noted that at the injection point there are present all the possible values for the phase-shift. This happens because the electric field has a node in such a point while the self-consistent field pushes outward the electrons in all radial directions. The phase-shift acquire mostly the values

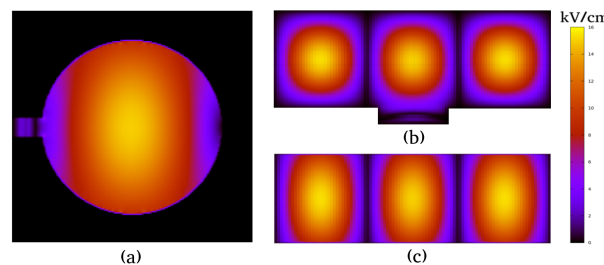


Figure 6: Steady-state electric field distribution in (a) the cross section $z = L_c/2$, (b) the longitudinal plane $y = 0$ and (c) the longitudinal plane $x = 0$.

around of the value $\pi/2$ due to the deviation produced by the magnetic field component of the microwave field [12]. Then a fast phase-focalization occurs by the microwave field at the position $z \approx 5 \text{ cm}$, where all the electrons are close to the exact resonance, $\varphi = \pi$. We can see that the phase shift

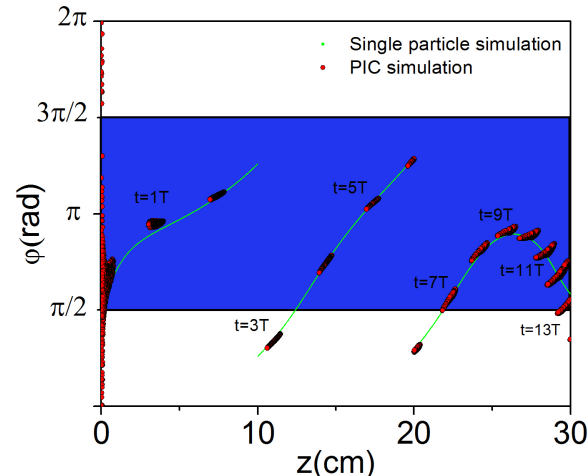


Figure 7: Time evolution of the phase-shift between the electrons transversal velocities and the right-hand circular polarized component of the electric microwave field. Red circles correspond to the case of $n_e = 10^8 \text{ cm}^{-3}$ electrons bunched and the green line for the single particle approximation.

φ jumps an angle π at the planes $z = 10 \text{ cm}$ and $z = 20 \text{ cm}$, where the TE_{113} microwave electric field has nodes (see Fig. 6). These jumps don't remove significantly the phase-shift from the *Acceleration band* $\pi/2 < \varphi < 3\pi/2$; therefore the electrons energies grow monotonously, except for the regions $10 \text{ cm} \leq z \leq 12.5 \text{ cm}$ and $20 \text{ cm} \leq z \leq 22.5 \text{ cm}$ where the φ values are outside of the *Acceleration band* (see Fig. 8). From this figure we can see that there is not any significant difference between the energy evolution of both the electrons bunched and the single electron. It can be noted in Fig. 7, Fig. 8 and Fig. 9 that its projections onto the z -axis are intervals of the width about of 1 cm, the diameter of the electrons bunched. For this case, the self-consistent field

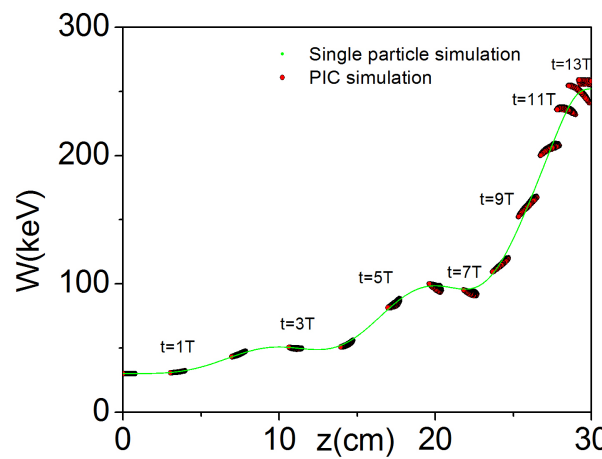


Figure 8: Time evolution of the energy for the $n_e = 10^8 \text{ cm}^{-3}$ electrons bunched (red circles) and for the single particle approximation (green line).

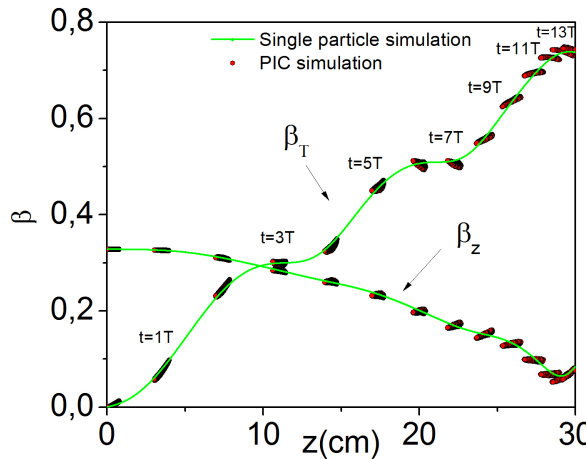


Figure 9: Time evolution of the transversal ($\beta_T = v_T/c$) and longitudinal ($\beta_z = v_z/c$) velocities for the $n_e = 10^8 \text{ cm}^{-3}$ electrons bunched (red circles) and for the single particle approximation (green line).

does not significantly affect the electron-beam focalization (see Fig. 7) and the energy spread of the electrons impacting on the wall is found not greater than 8% (see Fig. 8).

The evolutions of the transversal and longitudinal velocity components are shown in Fig. 9. It can be noted the diamagnetic force effect on the longitudinal velocity, which decrease until the value $0.08 c$ when the electrons impact to the cavity. In such position the transversal velocity of the electrons is maximum.

For case 2 (see Table 2), the bunch evolution is found similar to described in case 1; except for times greater than 5 microwaves period (see Figs. 8 and 11). This effect is

attributed to the self-generated electric field, \vec{E}^{sg} ; which is 10 times more intense than for the case 1. The self-generated electric field tends to expand the electrons bunch in all radial directions; however, in the transversal plane, the combined effect of the microwave electric field component \vec{E}^{hf} and the magnetostatic field contribute to the transversal confinement of the electrons bunch. On the contrary, in the axial direction, there is not any confinement mechanism for the electrons bunch; which causes its widening in such direction. It can be appreciated in Figs. 8 and 11 that its projections onto the z-axis are intervals of the width about of 3 cm and 4 cm, for the instants $t = 7$ and $t = 9$ microwaves periods, respectively. Such widening causes a spread in the velocities

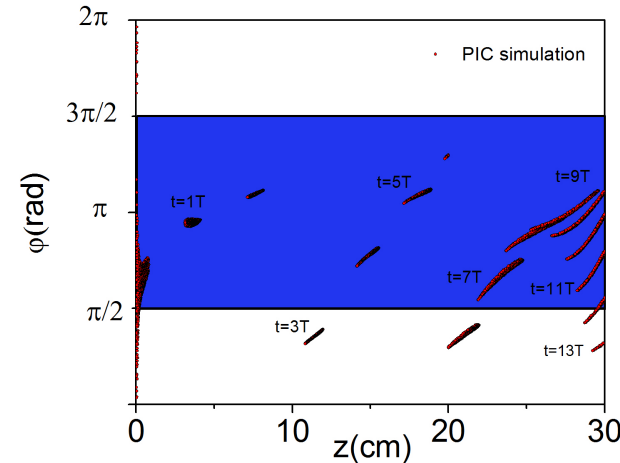


Figure 10: Time evolution of the phase-shift between the electrons transversal velocities and the right-hand circular polarized component of the electric microwave field for the $n_e = 10^9 \text{ cm}^{-3}$ electrons bunched.

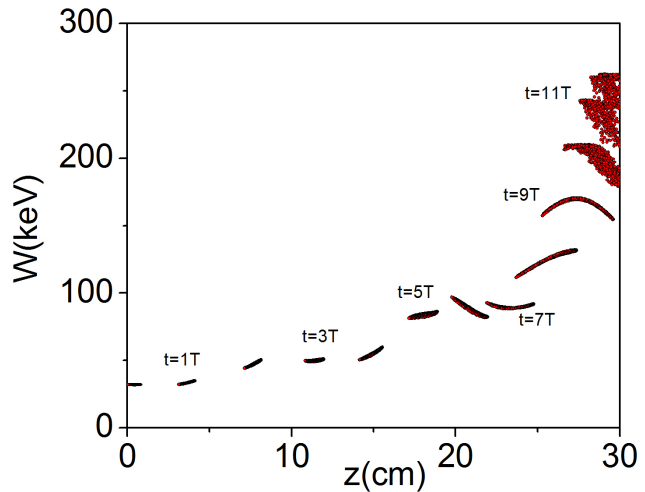


Figure 11: Time evolution of the energy for the $n_e = 10^9 \text{ cm}^{-3}$ electrons bunched.

of the electrons move in different acceleration conditions (see Fig. 10 for $t \geq 9$ microwaves period). The energy spread observed in Fig. 11 is caused by this effect.

We can note that the spread in the velocity is found similar for both, the longitudinal and transverse velocity (see Fig. 12).

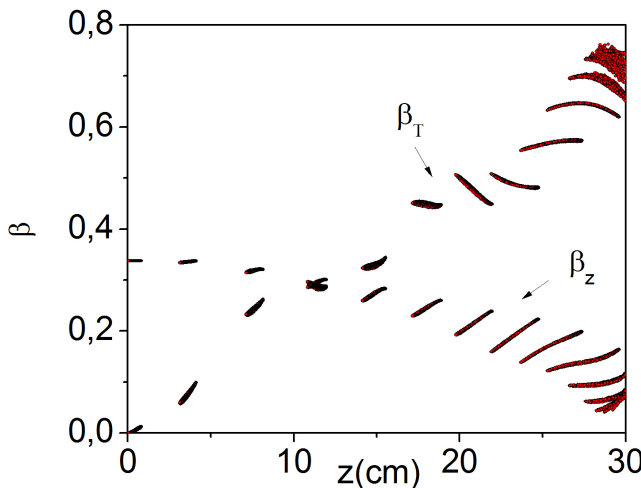


Figure 12: Time evolution of the transversal ($\beta_T = v_T/c$) and longitudinal ($\beta_z = v_z/c$) velocities for the $n_e = 10^9$ electrons bunched.

Figure 13 shows the energy spectrum of the electrons that impact with the opposite wall of the cavity at the position $z = L_c$ obtained from our numerical simulations for the two cases considered (see Table 2). We can note that the energy spread for the $n_e = 10^8 \text{ cm}^{-3}$ electrons bunches is not greater than 8%.

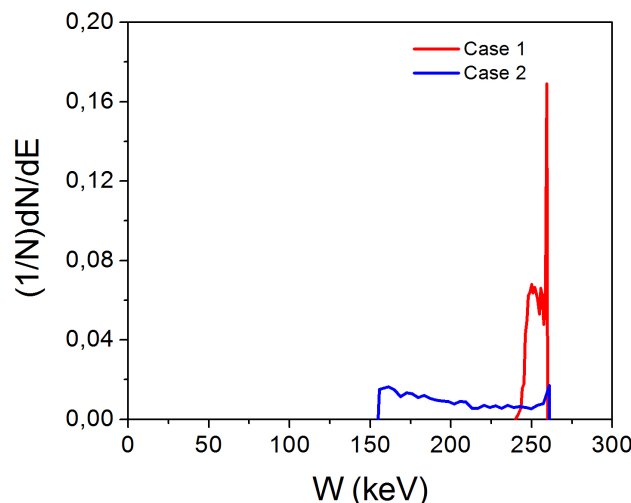


Figure 13: Numerical predictions of the energy spectrum for the electrons impacting on the cavity wall, $z_{wall} = L_c$, for the $n_e = 10^8 \text{ cm}^{-3}$ electrons bunched (red line) and for the $n_e = 10^9 \text{ cm}^{-3}$ electrons bunched (blue line).

CONCLUSION

The realized numerical experiment shows that electrons bunched can be accelerated up to energies of 250 keV in spatial autoresonance acceleration conditions by using a TE_{113} mode. It was shown that for the $n_e = 10^8 \text{ cm}^{-3}$ electrons bunch there is not present serious defocalization effect. For the $n_e = 10^9 \text{ cm}^{-3}$ electrons bunched, the self generated electric field spread it in longitudinal direction, which affect the acceleration regime. However, this effect can be reduced by using a continuous electron beam in the injection process.

REFERENCES

- [1] H. Gardner, T. Ohkawa, A. Howald, A. Leonard, L. Peranich, and J. D'Aoust, "An inexpensive x-ray source based on an electron cyclotron", *Review of Scientific Instruments*, vol 61, no 2, pp. 724-727, 1990.
- [2] R. Baskaran and T. Selvakumaran, "Studies on enhancement of x-ray flux in the compact electron cyclotron resonance plasma x-ray source", *Review of Scientific Instruments*, vol 71, no 2, pp. 1203-1205, 2000.
- [3] R. Symons, J. Hirshfield, and C. Wang, "Multi-stage cavity cyclotron resonance accelerator", U.S. Patent and Trademark Office No. 6,914,396, Jul. 31, 2005.
- [4] T. Inoue, T. Hattori, S. Sugimoto, and K. Sasai, "Design study of electron cyclotron resonance-ion plasma accelerator for heavy ion cancer therapy", *Review of Scientific Instruments*, vol 85, no 2, p. 02A958, 2014.
- [5] V. Andreev, D. Chuprov, V. Ilgisonis, A. Novitsky, and A. Umnov, "Gyromagnetic autoresonance plasma bunches in a magnetic mirror", *Physics of Plasmas*, vol 24 no 9, p. 093518, 2017.
- [6] A. Kolomenskii and A. Lebedev, "Self-Resonant Particle Motion in a Plane Electromagnetic Wave", *Doklady Akademii Nauk*, vol 145, no 6, pp. 1259-1261, 1962.
- [7] V. Davydovskii, "Possibility of Resonance Acceleration of Charged Particles by Electromagnetic Waves in a Constant Magnetic Field", *Sov. Phys. JETP*, vol 16, pp. 629-630, 1963.
- [8] R. Shpitalnik, C. Cohen, F. Dothan, and L. Friedland, "Autoresonance microwave accelerator", *Journal of applied physics*, vol 70 no 3, pp. 1101-1106, 1991.
- [9] L. Friendland, "Spatial autoresonance cyclotron acceleration", *Physics of plasmas*, vol 1, no 2, pp. 421-428, 1994.
- [10] K. Golovanivsky, "Autoresonant acceleration of electrons at nonlinear ECR in a magnetic field which is smoothly growing in time", *Physica Scripta*, vol 22, no 2, pp. 126-133, 1980.
- [11] O. Gal, "GYRAC: a compact, cyclic electron accelerator", *IEEE Transactions on Plasma Science*, vol 17, no 4, pp. 622-629, 1989.
- [12] V. Dugar-Zhabot and E. Orozco, "Cyclotron spatial autoresonance acceleration model", *Physical Review Special Topics-Accelerators and Beams*, vol 12, no 4, p. 041301, 2009.
- [13] V. Dougar-Jabon, E. Orozco, and A. Umnov, "Modeling of electron cyclotron resonance acceleration in a stationary inhomogeneous magnetic field", *Physical Review Special Topics-Accelerators and Beams*, vol 11, no 4, p. 041302, 2008.

- [14] V. Dugar-Zhabon, J. González, and E. Orozco, “3D electromagnetic simulation of spatial autoresonance acceleration of electron beams”, in *Journal of Physics: Conference Series*, vol 687, no 1, p. 012077, 2016.
- [15] V. Vergara, J. González, J. Beltrán, and E. Orozco, “Electrons acceleration in a TE_{113} cylindrical cavity affected by a static inhomogeneous magnetic field”, in *Journal of Physics: Conference Series*, vol 935, no 1, p. 012076, 2017.
- [16] V. Dugar-Zhabon, E. Orozco, and A. Herrera, “Self-consistent simulation of an electron beam for a new autoresonant x-ray generator based on TE_{102} rectangular mode”, in *Journal of Physics: Conference Series*, vol 687, no 1, p. 012076, 2016.
- [17] V. Milant'ev, “Cyclotron autoresonance—50 years since its discovery”, *Physics-Uspekhi*, vol 56, no 8, pp. 823-832, 2013.
- [18] V. Dugar-Zhabon and E. Orozco, “Compact self-resonant X-ray source”, U.S. Patent and Trademark Office No. 9,666,403,
- May 30, 2017.
- [19] R. Hockney and J. Eastwood, *Computer simulation using particles*. Bristol: Hilger, 1988.
- [20] A. Taflove and S. Hagness, *Computational Electrodynamics: The Finite-Difference Time-Domain Method in Electromagnetics*. Norwood, MA: Artech House, 2000.
- [21] K. Yee, “Numerical solution of initial boundary value problems involving Maxwell's equations in isotropic media”, *IEEE Transactions on antennas and propagation*, vol 14, no 3, pp. 302-307, 1966.
- [22] T. Umeda, Y. Omura, T. Tominaga, and H. Matsumoto, “A new charge conservation method in electromagnetic particle-in-cell simulations”, *Computer Physics Communications*, vol 156, no 1, pp. 73-85, 2003.